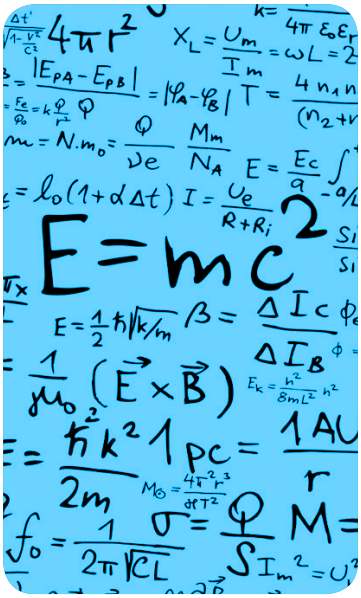

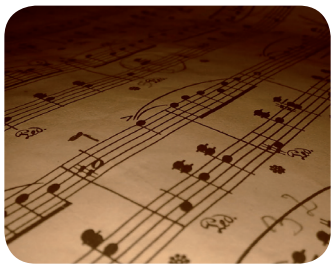

MÁSTERES de la UAM

Facultad de Ciencias /11-12

Máster en Nanociencia y Nanotecnología Molecular.

UNIVERSIDAD AUTONOMA DE MADRID

excelencia Campus Internacional UAM CSIC

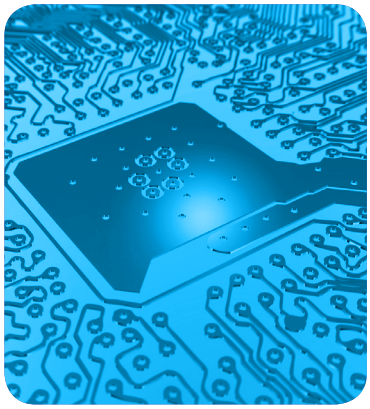

Patterned conductive nanostructures from reversible self-assembly of 1D coordination polymner

Mohammad-Reza Azani

UAM EDICIONES

Aknowledgments

I would like to express my gratitude to my research advisors Prof. Felix Zamora and Dr. Ruben Mass-Balleste for their support have lead me to complete this thesis.

Specific thanks must be given to Prof. Tomas Torres as a coordinator of the master for his guidance and attentions.

I would also like to thank Prof. Massimiliano Cavallini, Denis Gentili, Gonzalo Givaja, Arian Shehu, Francesca, Leonardi and Eva Mateo-Martí, Pierpaolo Greco for doing Nanolithography and its measurements.

I would also like to thank the faculty and staff of UAM Inorganic and Organic Chemistry Departments and the Investigation Service of the University for their Excellent Work.

I would like to thank the members of my graduate committee Prof. Tomás Torres, Prof. Fernando Langa, Prof. Christian Claessens, Prof. Roberto Otero for their time and support.

Also, I am grateful to all the postgraduate students of whom I got to know during my stay at the department.

I would also like to thank my family for the support they provided me through my entire life and in particular, I must acknowledge my wife and best friend, Azin Hassanpour, without whose love, encouragement and assistance, I would not have finished this thesis.

Thank you all.

Abstract

The present study is aimed at elucidating the factors that govern the spontaneous assembly of a family of coordination polymers called MMX $[Pt_2(S_2CR)_4I]$ in solution and use these materials to prepare patterned conductive nanostructures. In solution, according to spectroscopic evidences, we observed different species $[Pt_2(S_2CR)_4]$ and $[Pt_2(S_2CR)_4I_2]$ at room temperature and also assembly of these species at low temperatures. A set of experiments allowed to determine the effect of temperature, concentration, solvent and the nature of ligand on assembly of species. The reversible self-organization from solution allowed us to generate highly electrical conductive structures located upon demand on technologically relevant surfaces, by easy-to-handle and low cost micromolding in capillaries (MIMIC) and lithographically controlled wetting (LCW). Electrical characterization reveals a near Ohmic behaviour and a high stability of the stripes (in air). Nanolithography techniques from a solution of these CP demonstrated that this material can be efficiently used as a molecular wire.

Table of Contents

Introduction

The assembly of molecules, biological materials and nanoparticles in ordered superstructures on solid surfaces is of great interest in many areas of science and technology.[1,2] Supramolecular chemistry,[3] exploring self-assembly beyond single molecular entities, has provided remarkable results, but in order to embed these supramolecular structures in real applications it is necessary to gain control over their intimate spatial architecture, from the molecular scale to the macro scale. The exploitation of self-assembly properties in bottom-up nanofabrication has been demonstrated as a successful strategy towards these aims.[3,4] A major challenge in miniaturized device fabrication is to enhance performance by taking advantage of selected features of materials. Therefore, the application of advanced techniques able to exploit self-organizing properties of materials is essential for the construction of devices based on supramolecular constituents.[4–6] Self-organizations promoted by non-covalent interactions have been extensively studied in solution, in the solid state and on surfaces, leading to a large variety of supramolecules with different architectures.[7] Some of these supramolecules have been designed using coordinative bonds.[8] By means of coordinative bonds, infinite associations between two simple building blocks, metal entities and organic or inorganic ligands have led to the formation of a large number of architectures of different dimensionalities,[9] which are known as coordination polymers (CPs). The kinetic lability of metal–ligand bonds[10] supports the reproducible construction of functional, highly ordered superstructures for a wide range of technological applications (i.e. catalysis, reaction confinement, gas storage and separation).[6,11–14] Coordination polymers show interesting chemical[14] and physical[15] properties, including high electrical conductivity.[16] Current interest in the development of highly conductive CPs is also motivated by their potential technological impact.[17] A relevant example concerning the electrical conductivity of CPs is the so-called MMX chains. The structure of an MMX chain can be described as a pseudo-one-dimensional arrangement of halides (X) bridging dimetallic subunits, in which metal ions are connected by ligands (e.g. pyrophosphates or dithiocarboxylates) (Scheme 1).

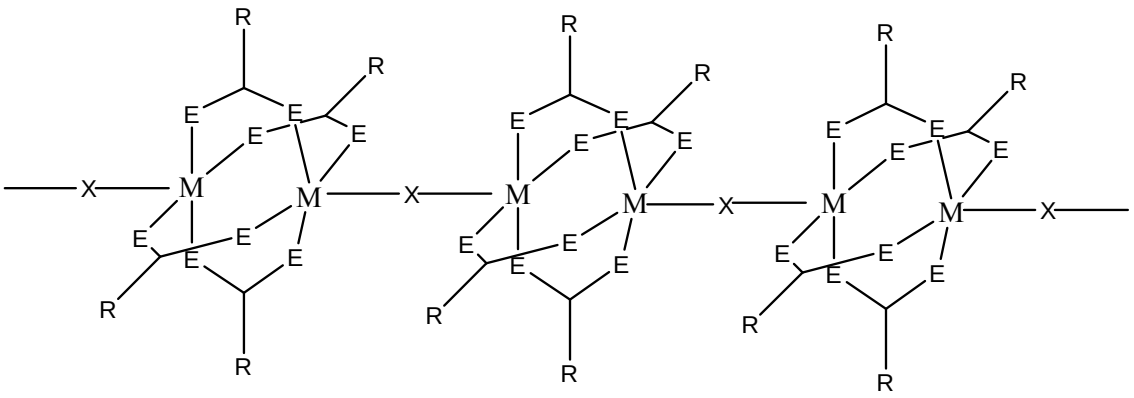

Scheme 1. The structure of an MMX as a pseudo-one-dimensional arrangement. (M=Pt, Pd E=O,S R= different groups and X=I, Br, Cl).

The MMX chains based on platinum, dithiocarboxylate and iodine have shown metallic conductivity at room temperature. They are promising candidates for nanoelectronic applications, where molecular wires capable of transporting electrical charges across long distances are required.[17]

Furthermore, the relatively low work function (about 3.7 eV)[18] and the fact that thin films of MMX are almost transparent in thickness, <50 nm, make this class of CPs extremely appealing for molecular electronics and optoelectronics. Recently, our group has shown the outstanding electrical properties of randomly deposited MMX nanoribbons and nanocrystals ($[Pt_2(RCS_2)_4I]_n$, R = methyl or n-penthyl) on mica.[18,19] However, the conductive nanoribbons were formed on mica by direct sublimation from crystals of $[Pt_2(methyl\text{-}CS_2)_4I]n$ under a high vacuum.[20] This method does not allow spatial control of the deposition of nanoribbons on surfaces. Once the conductivity of nanostructures of such CPs has been demonstrated, the next frontier is to fabricate a functional device based on this polymer. To address this challenge, we evaluated the processability of such a polymer. Being demonstrated an outstanding ability for reversible depolymerization/repolymerization, we envisioned the possibility of integrating a CP self-assembly in a spatially confined environment by unconventional wet lithography,[21] exploiting its depolymerization/repolymerization ability.[10]

Results and discussion

a) Species in the solution at Room Temperature.

A significant feature of of $[Pt_2(RCS_2)_4I]_n$ (R= n-butyl (**1**), n-pentyl (**2**), Iso-butyl (**3**)) (scheme. 2) is their processability. Indeed, it is very uncommon that a coordination polymer can be dissolved and recrystallized conserving its structural integrity.[16] However, this characteristic is what allowed us to design devices based on local crystallization of polymer **1** from CH_2Cl_2 solutions. In fact, this uncommon behaviour raises the questions of which species are present in solution and which factors have an effect on their subsequent reassembly.

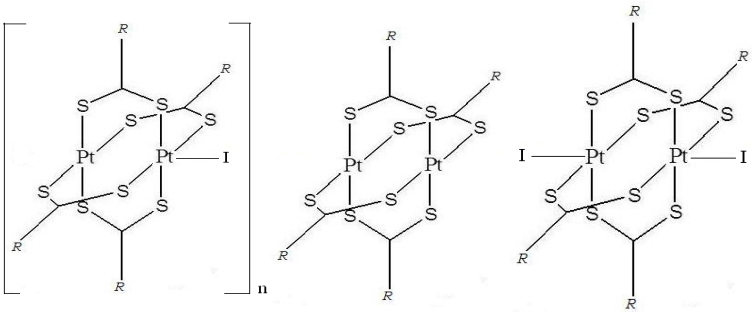

(1) (2) (3) **(4) (6) (8)** **(5) (7) (9)**

R	MMX	MM	XMMX
$(CH_2)_3CH_3$	(1)	(4)	(5)
$CH_2CH(CH_3)_2$	(2)	(6)	(7)
$(CH_2)_4CH_3$	(3)	(8)	(9)

Scheme 2 The structure of $[Pt_2(RCS_2)_4I]_n$ (R= n-butyl (1), n-pentyl (2), Iso-butyl (3)) and their precursors units.

In order to address these important unknown factors, we analysed the spectroscopic features of **1** dissolved in CH_2Cl_2 and compared them with those of the $[Pt_2(nBuCS_2)_4]$ (**4**) and $[Pt_2(nBuCS_2)_4I_2]$ (**5**) precursors. The data shows that, at room temperature, **1** dissolved in an equimolar mixture of **4** and **5**. The UV-vis spectrum of a 1 mM solution of **1** can be seen as the result of overlapping the UV-vis spectra separately measured from 0.5 mM CH_2Cl_2 solutions of precursors **4** and **5** (Fig. 1). Consistently, the 1H NMR spectrum of 1 in CD_2Cl_2 shows an overlapping of the spectra of species **4** and **5** precursors (Fig. 2). The spectroscopic data indicate an asymmetric rupture of 1, which formed two different diamagnetic dimetallic compounds containing two Pt(II) centres (in the case of **4**) or two Pt(III) centres (**5**). For **2** and **3** we observed

the same behavior which formed two different species **6**,**7** and **8**,**9** respectively in CH_2Cl_2.

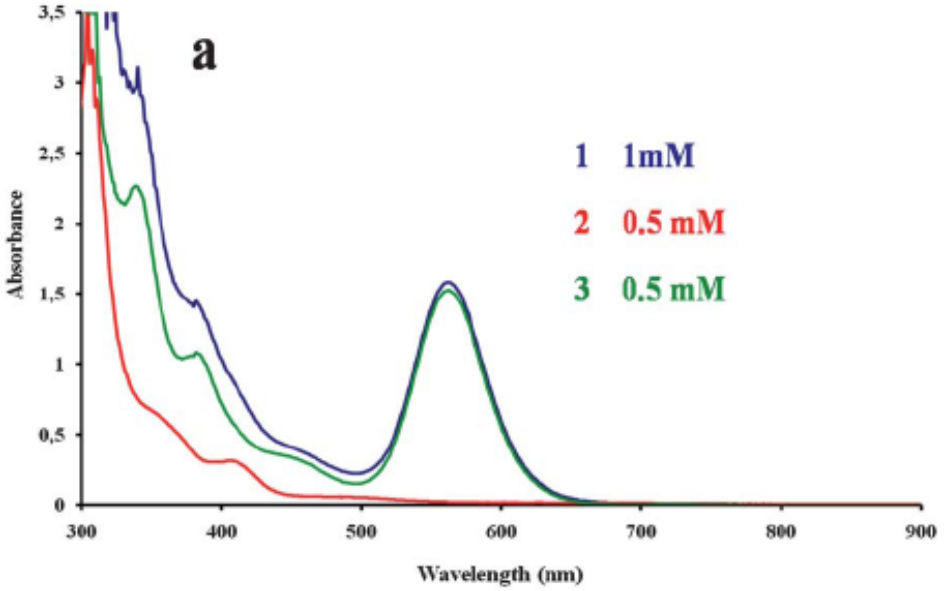

Fig. 1 Spectroscopic studies of $[Pt_2(nBuCS_2)_4I]n$ (1) in CH_2Cl_2. UV-vis at room temperature..

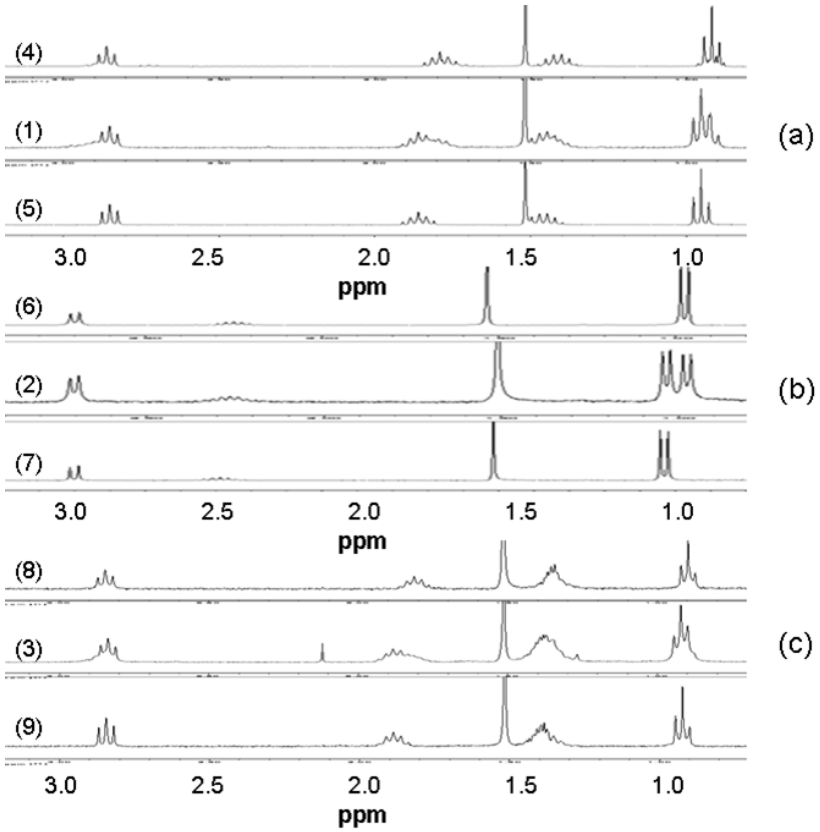

Fig .2 The ^1H NMR spectrum of **1** (a) ,2 (b) ,3 (c) and also their pure precursors in CD_2Cl_2 at room temperature.

The ^{1}H NMR spectrum of **1-3** in other solvents such as $CHCl_3$ and CS_2 also were explored at room temperature. The results have shown the same behaviors that we have observed in the CH_2Cl_2. (Fig 3).

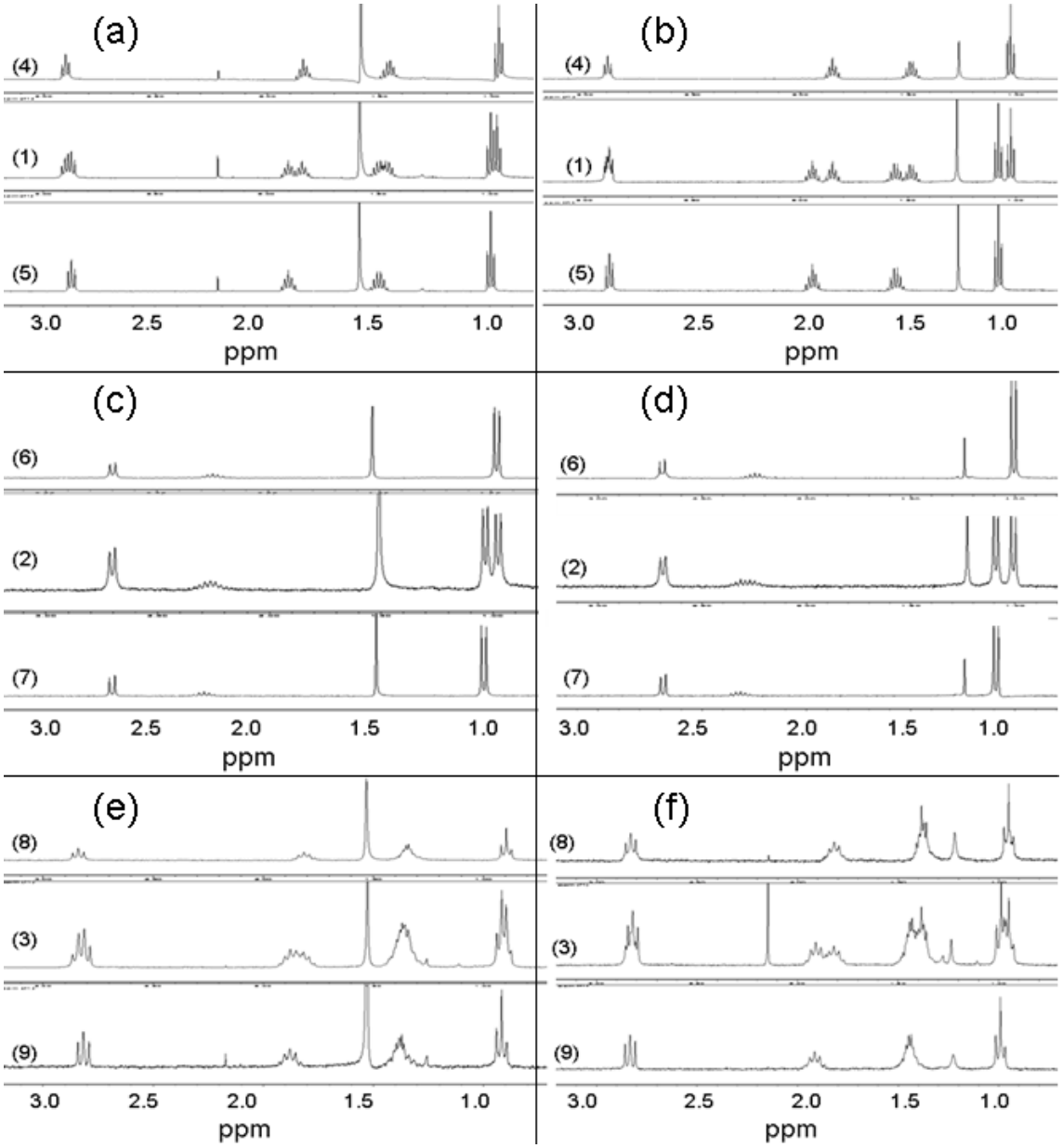

Fig .3 The ^{1}H NMR spectrum of **1** in $CDCl_3$ (a) and CS_2 (b) , **2** in $CDCl_3$ (c) and CS_2 (d) and **3** in $CDCl_3$ (e) and CS_2 (f) and also their pure precursors at room temperature.

So in the solutions with different solvents and ligands we observed the same behaviors. In fact all the MMX units in the solutions dissociation into their precursors MM and XMMX at room temperature. (Scheme 3).

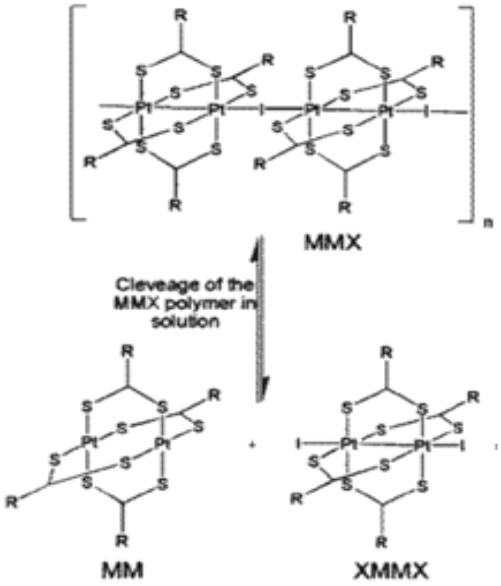

Scheme 3 A schematic representation of the behaviour observed for the solutions of **1-3** in different solvents at room temperature.

b) Supramolecular assembly of compounds 1, 2 and 3: Effect of Concentration and Temperature.

Concerning the (re)assembly of 4 and 5, as previously observed for analogous species,[22] precursor 4 associated in solution via reversible weak d8…d8 interactions, which can be observed by the appearance at low temperature of an adsorption band at 600–700 nm. Similar behaviour was observed for the solutions of 1. In addition, a new band at 820 nm appeared in the spectrum of 1 in CH_2Cl_2 at -50 ºC (Fig. 4). Considering that this feature was not observed for the solutions of pure precursors 4 or 5, this new band indicates the assembly of molecules 4 and 5, generating oligomers of polymer 1.
We also have observed the same behaviours in 2, 3. A schematic representation of the behaviour observed for the solutions of 1-3 in CH_2Cl_2 at low temperature was shown in Scheme 4.

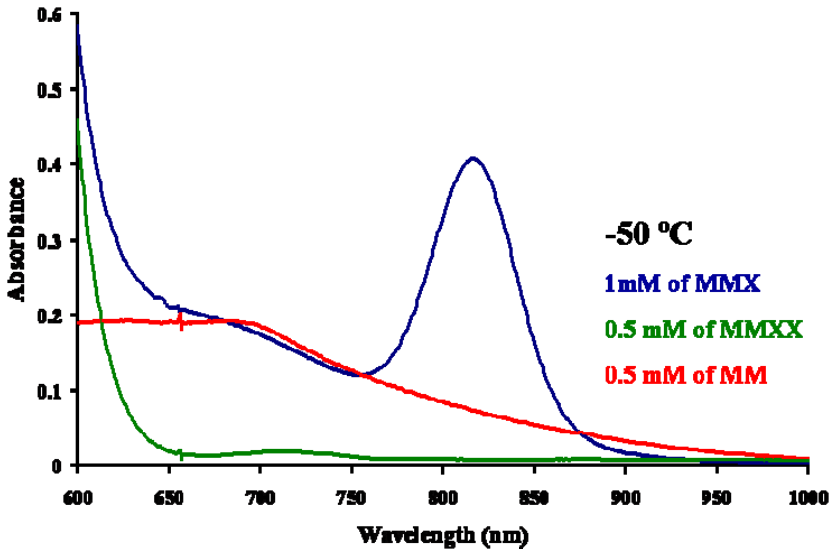

Fig. 4 UV-vis spectrum of a 1 mM solution of $[Pt_2(n\text{BuCS}_2)_4I]_n$ in CH_2Cl_2, compared with UV-vis spectra of 0.5 mM solutions of $[Pt_2(n\text{BuCS}_2)_4]$ and $[Pt_2(n\text{BuCS}_2)_4I_2]$ in CH_2Cl_2. All data was taken at -50.

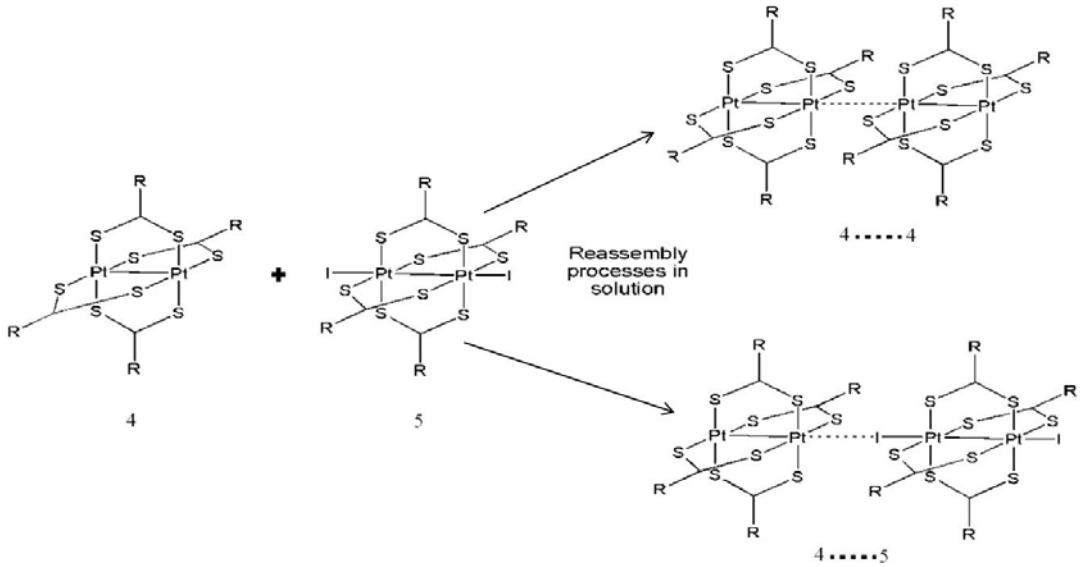

Scheme 4 A schematic representation of the behaviour observed for the solutions of **1-3** in different solvents at room temperature.

Interestingly, the ratio between the 4….4 and the 4…...5 association was affected by the overall concentration of dissolved 1, in that the 4….4 assembly was less favoured at lower concentrations (Fig. 5).

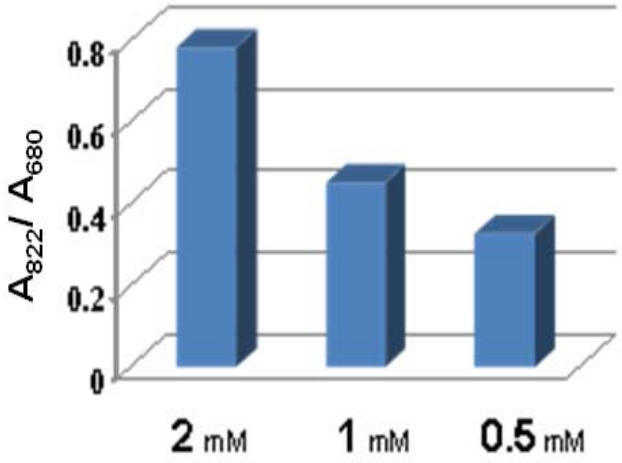

Fig. 5 The ratio between MM···MM and MM···XMMX assemblies depends on the concentration. At higher concentrations the relative amount of MM···MM suprastructures increases. (**1** in different concentration in CH_2Cl_2).

c) Supramolecular assembly of compounds 1, 2 and 3: Effect of ligand.

Effect of ligand can be primarily discussed regarding the results obtained in CH_2Cl_2 (Fig.6). Temperature dependence of the molar absorptivity of signals at around 700 nm and 820 nm that appears at low temperatures in 1 mM solutions of **1-3** was shown in Fig. 7. Behavior of compounds **1-3** can rationalize in terms of effective bulkiness in solution of dithiocarboxylato ligand. When ligand contains a ramified R group (compound **2**) the approaching of bimetallic units especially in 700 nm reagion that is related to MM aggrigations is definitively more difficult than compounds **1** and **3** which contain linear R groups. Between **1** and **3** supramolecular assemblies are favored for **1**, because R is a shorter chain.

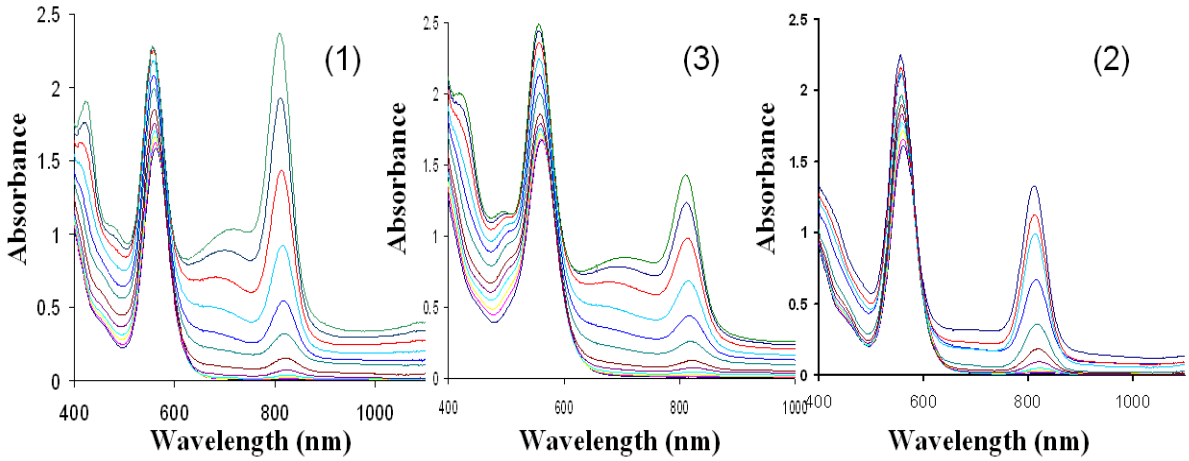

Fig. 6 UV-vis spectrum of a 1 mM solution of 1,3 in CH_2Cl_2 (from 20 ºC to -90) and 2 (from 20 ºC to -80)

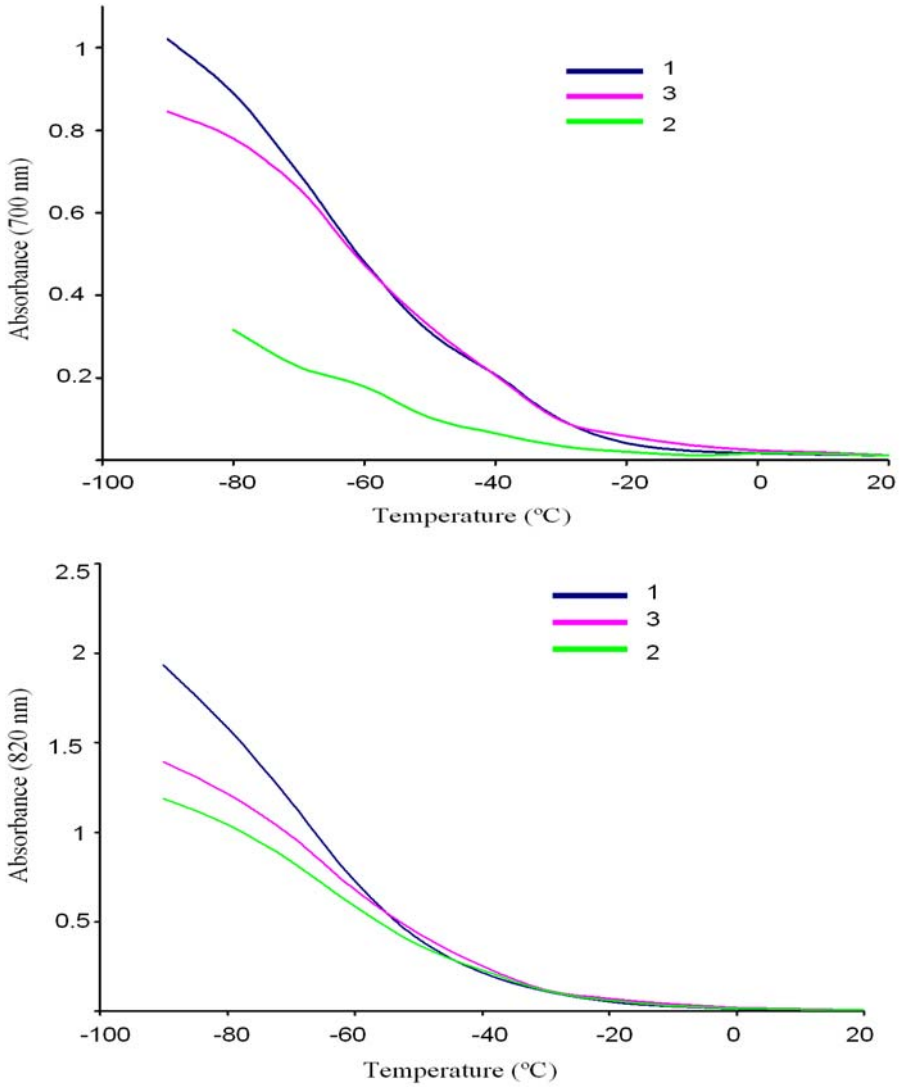

Fig. 7 The temperature dependence of the molar absorptivity of signals at 700 nm (a) and 820 nm (b) that appears at low temperatures in 1 mM solutions of **1-3** in CH_2Cl_2.

d) Supramolecular assembly of compounds 1-3 in $CHCl_3$, THF and CS_2: Effect of solvent.

The effect of solvent in self-assembly of compounds **1-3** in solution has been examined comparing the behaviour of solutions using as a solvent CH_2Cl_2, $CHCl_3$, THF and CS_2. However, to compare the inherent ability of compound **1-3** to associate in solution in different solvents, unique conditions (the same concentration) such as shown in Fig.8 have to be used. Compounds **1-3** show comparable trends. Thus, at the same conditions, while certain degree of self-assembly in CH_2Cl_2 and $CHCl_3$ is observed, CS_2 and THF hamper the association in solution. This effect can be easily justified considering the known coordinative ability of such solvents, which can result in weak

metal-ligand interactions between the solvent molecules and the Pt(II) centers, which make more difficult self-assembly of 4…4 in the 700 nm region through Pt···Pt interactions and for assembly of 4…5 about 820 nm in compound **1**. Notwithstanding this, in THF as a less coordinating solvent in comparison with CS_2, when the temperature is low enough; new features in the lower energies region appear, indicating certain degree of self-assembly.

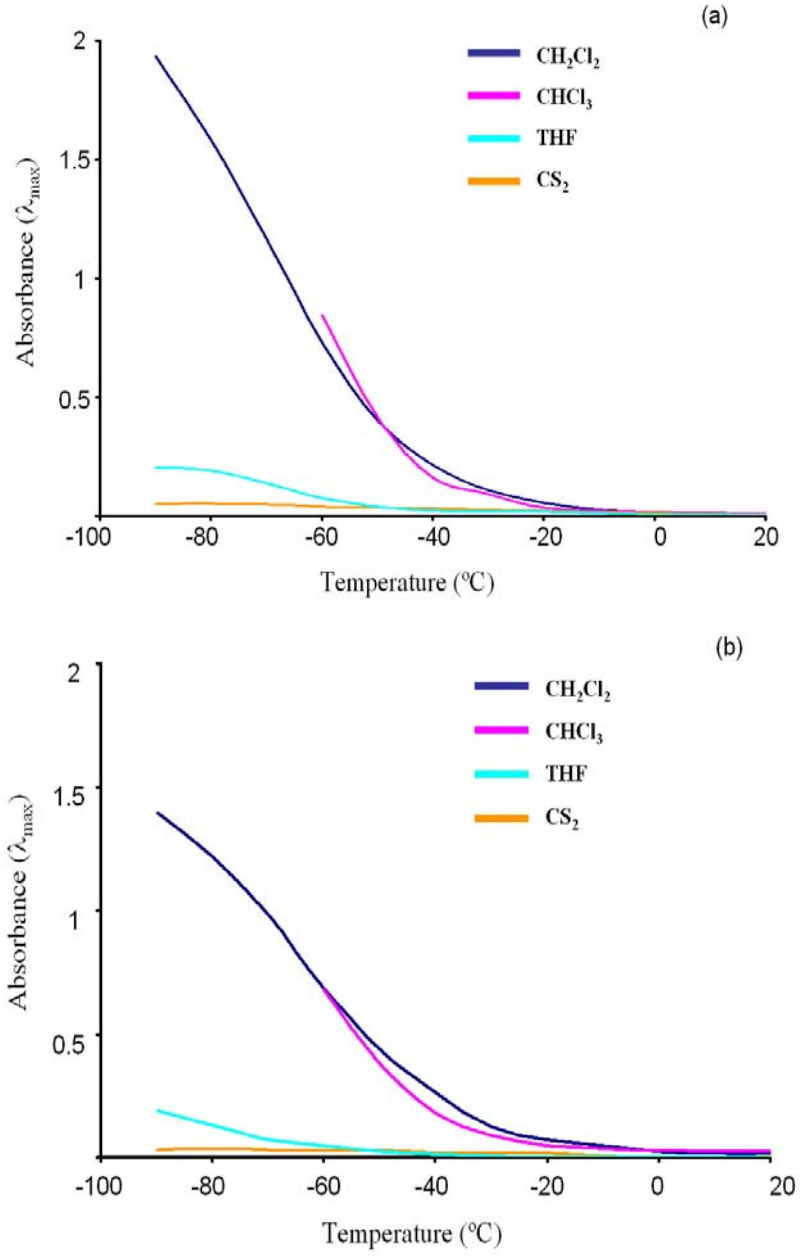

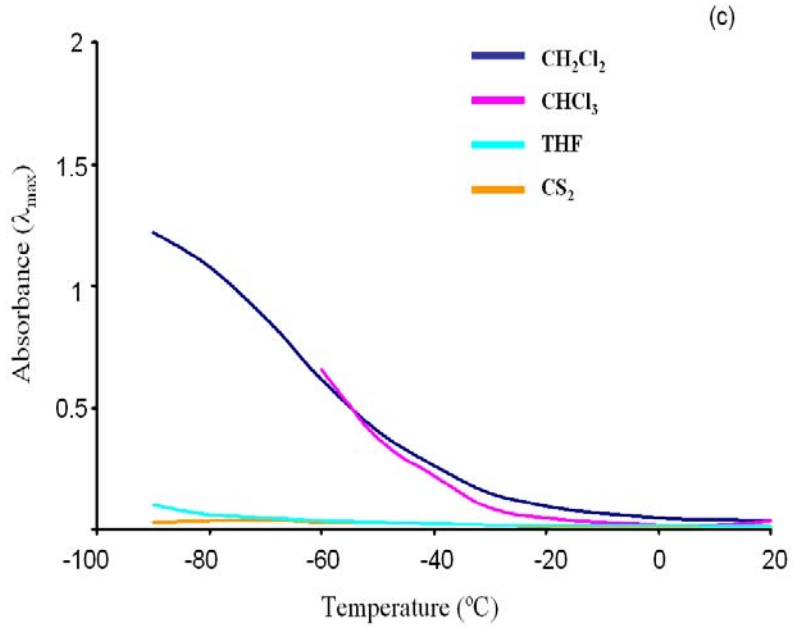

Fig. 8 Effect of different solvents on 1mM solution of 1(a), 2(b) and 3 (c).(for each solvent we considered the max Abs. near 820 nm)

e) Formation of patterned conductive nanostructures by Nanolithography

The key factor for the processability and the successful application of MMX as an electrode is its excellent reversibility in the depolymerization/repolymerization process. Thus, micromolding in capillaries (MIMIC)[23] and lithographically controlled wetting (LCW)[24] in Fig. 9 were used to fabricate ordered patterns of parallel sub-micrometric wires (μ-wires).

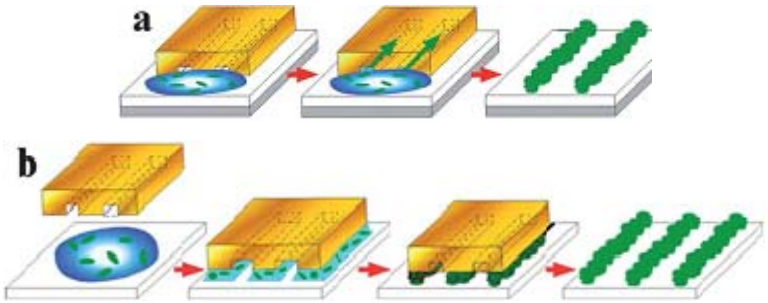

Fig. 9 (a) A schematic representation of micromolding in capillaries (MIMIC). After vacuum sublimation (right in upper row) of pentacene this procedure allowed us to form the microstructure and electrodes of a field effect transistor. (b) A schematic representation of lithographically controlled wetting (LCW).

Noticeably, both methods were able to deliver a solution at spatially controlled positions, exploiting the self-organization properties of the solute at the later stages of shrinking, leading to the formation of patterned superstructures.[25] Fig. 10 shows an optical micrograph of μ-wires and parallel μ-wires (width 900 nm, height 124 nm,

periodicity 1.5 μm) on pre-fabricated gold electrodes that were printed by MIMIC. Morphological characterizations were shown in Figs 11,12.

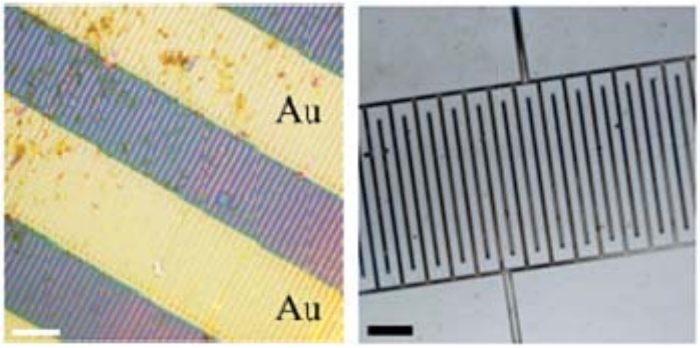

Fig. 10: Microfabrication by unconventional wet lithography. An optical image (scale bar = 10 μm) of parallel m-wires printed onto Au surface (right). An optical micrograph (scale bar = 100 μm) of interdigitated comb-like electrodes of $[Pt_2(nBuCS_2)_4I]_n$ printed on silicon oxide by LCW (left).

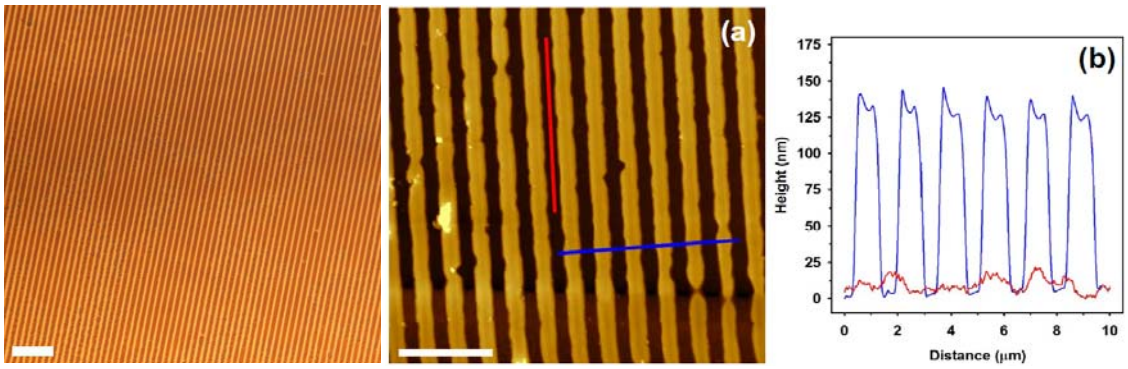

Fig. 11 a) AFM morphology (scale bar = 5 μm), and b) AFM profiles of $[Pt_2(nBuCS_2)_4I]_n$ wires patterned on gold electrodes (LCW, parallel lines, 2 mg/mL in CH_2Cl_2)

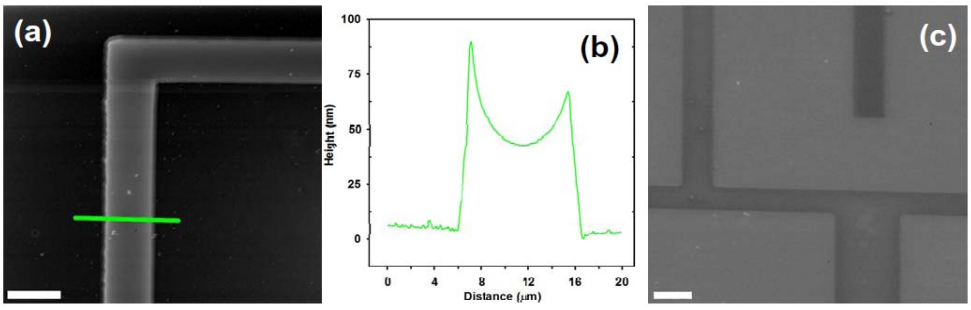

Fig. 12 a) AFM image (scale bar = 10 μm), b) AFM profile, and c) SEM (scale bar = 10 μm) of $[Pt_2(n\text{BuCS}_2)_4I]_n$ pattern on silicon oxide (LCW, interdigitated comb-like, 2 mg/mL in CH_2Cl_2).

The electrical characterization was performed by measuring the current flowing in the μ-wires as a function of bias voltage, ranging from +50 to -50 V. The I–V curve (Fig. 12) reveals a near Ohmic behaviour within the range explored.

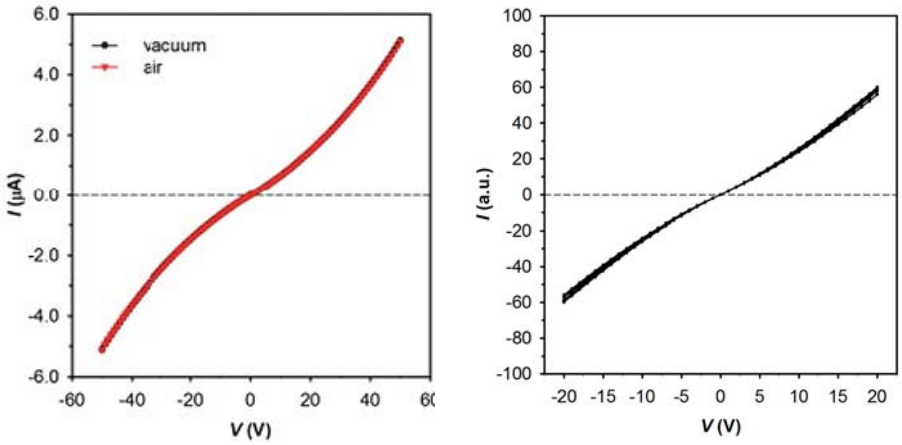

Fig. 12 Current vs. voltage characteristics of the wires in (left). Current *vs* voltage characteristic upon the application of 10 cycles on wires patterned on gold electrodes after 6 month (right).

It is important to note that the time stability of the wires (we tested our devices for more than 6 months, in air at room temperature and in high humidity), in terms of their electrical behaviour, was not influenced by air and was consistently reproduced in ten voltagesweeping cycles (Fig.12). Indeed, the data points acquired in both the vacuum and air fell on top of each other, showing no sign of hysteresis or any other electrical deterioration. This is a very important issue for electronic applications. Assuming that the current spreads across the entire section of the wires of 1, we estimated a high current density of ca. 5 A cm^{-2} at 50 V, which for sub-micrometric wires is comparable to and, in some cases, even better than corresponding metallic wires.[6,26]

Conclusions

The data presented herein demonstrates the unusual ability of **1**-**3** chains to reversibly assemble and disassemble in solution into their structural building blocks, **4,5** and **6,7** and **8,9** respectively. Also the results presented were shown the effect of some factors like the nature of ligands and solvents that have an influence on such self-organization. The smaller alkyl chain, not bulkier ligands and not coordinating solvents amplify the aggregation in both regions about 700 nm and 820 nm that are related to aggregations of species respectively. Ratio between M…M and XMMX…MM aggregations depend on concentration but also XMMX…MM is easier with bulkier ligands comparing with MM…MM. The outstanding features of polymer **1** in solution enable its processability by unconventional lithography. Thus, solutions of **1** were used to fabricate reliable sub-micrometric patterns for designing working electronic devices. The patterning of homogeneous structures from the sub-micrometric to the macro scale is a breakthrough, since CP properties critically depend on the uniformity at different length scales. In this respect, our work represents an important advance in view of the application of CPs in molecular devices and in organic electronics in general as molecular wires or as electrodes. As a consequence of the wet processability and excellent conductance of the MMX polymer, they can be considered a possible alternative to the traditional Au electrode in organic/hybrid devices, which can lead to the development of a new generation of devices based on CPs.

Experimental Section

Materials and Methods

Most of the reagents were purchased from Aldrich and used as received. CS_2 and Dichloromethane ≥99.9% were purchased from Sigma Aldrich and Scharlau respectively and used without further purification. Chloroform ≥99.95% and Tetrahydrofuran 99.9% were purchased from Carlo Erba Reactifs (SDS) and used without further purification.

The synthesis of dithicarboxylic acids**,** MM and XMMX precursors was carried out due to a procedure previously reported.[27] Spectroscopic characterization of compounds obtained was performed by means of Elemental analysis, IR, UV-vis and ^{1}H-NMR.

1H NMR spectras were recorded on a Bruker AMX-300 spectrometer. C, H, S elemental analyses were performed on aPerkin-Elmer 240-B microanalyzer. FTIR spectra (KBr pellets) were recorded on a Perkin-Elmer 1650 spectrophotometer. Electronic absorption spectrawere recorded on an Agilent 8452 diode array spectrophotometerover a 190–1100 nm range in 0.1, 0.2 and 1 cm quartz cuvettes thermostattedby a Unisoku cryostat.

Preparation of tetrakis(dithiobutanoato)diplatinum [Pt_2(n-ButCS_2)$_4$I] (1):

Compound **1** (55 mg, 0.06 mmol) was dissolved in 10 mL of toluene under reflux. To this strong reddish orange solution was added a solution of iodine (3.8 mg, 0.03 mmol) in 2 mL of toluene. On cooling with fridge, dark violet crystals with metallic luster separated from the resulting deep violet solution and were collected by suction filtration, washed with cold hexane and dried in vacuum. 53 mg (yield 84%). Analysis for [Pt_2(n-ButCS_2)$_4$I]: ($Pt_2S_8C_{20}H_{36}I$): Found: C, 21.6%; H, 3.6%; S, 23.5%. Calculated: C, 22.9%; H, 3.5%; S, 24.4 %.

Preparation of tetrakis(dithioiso-butanoato)diplatinum [Pt_2(Iso-ButCS_2)$_4$ I] (2):

Compound **2** (65 mg, 0.07 mmol) was dissolved in 10 mL of toluene under reflux. To this strong reddish orange solution was added a solution of iodine (4.4 mg, 0.035 mmol) in 2 mL of toluene. On cooling with fridge, dark violet crystals with metallic luster separated from the resulting deep violet solution and were collected by suction

filtration, washed with cold hexane and dried in vacuum. 58 mg (yield 80%). Analysis for [Pt_2(Iso-ButCS_2)$_4$I]: ($Pt_2S_8C_{20}H_{36}I$): Found: C, 22.1%; H, 3.6%; S, 24.0%. Calculated: C, 22.9%; H, 3.5%; S, 24.4%.

Preparation of tetrakis(dithiohexanoato) [Pt_2(n-PenCS_2)$_4$I] (3) :

Compound **3** (68.5 mg, 0.07 mmol) was dissolved in 10 mL of toluene under reflux. To this strong reddish orange solution was added a solution of iodine (4.4 mg, 0.035 mmol) in 2 mL of toluene. On cooling with fridge, dark violet crystals with metallic luster separated from the resulting deep violet solution and were collected by suction filtration, washed with cold hexane and dried in vacuum. 65 mg (yield 85%). Analysis for [Pt_2(*n*-PenCS_2)$_4$I]: ($Pt_2S_8C_{24}H_{44}I$): Found: C, 25.9%; H, 3.9%; S, 22.8%. Calculated: C, 26.1%; H, 4.0%; S, 23.2 %. IR (KBr, cm-1): 2922 (very strong), 2361 (strong), 1636 (strong), 1449 (strong), 1081 (medium). ^{1}H NMR (300 MHz, 298 K, CDCl3, $SiMe_4$) δ: 2.81 (m), 1.87 (m), 1.36 (m), 0.91 (m).

Lithographic methods

Solvents: The solutions were prepared using dichloromethane (Aldrich, anhydrous, ≥99.8%) and tetrahydrofuran (Aldrich, anhydrous, ≥99.9%).

Stamps: The elastomeric polydimethylsiloxane stamps (PDMS, Sylgard 184, Dow Corning) stamps were prepared by replica molding of a blank Compact Disk for parallel lines (periodicity of 1.5 μm, width at half height 500 nm and 220 nm deep), a photolithographic master for interdigitated comb-like microstructures and for OFET microelectrodes (two parallel lines with width at half height 500 μm and distance of 70 μm, provided by SCRIBA Nanotecnologie S.r.l.). PDMS stamps were cured for 6 h at 60°C, then peeled off and washed in pure ethanol for one hour.

Substrates: Si wafers (n-type doped) with 200 nm thermally grown SiO2 layer, borosilicate glass with 250 nm gold layer (ArrandeeTM, Germany), and microscope glass slides. All substrates were sonicated in electronic-grade water (milli-pure quality, 2 min), in acetone (Aldrich chromatography quality, 2 min), then in 2-propanol (Aldrich spectroscopic grade quality, 2 min), and blown dry in N2.

MIMIC: the stamp grooves placed in contact with the substrate (silicon oxide, glass, and gold surfaces) form capillary channels and $[Pt_2(n\text{BuCS}_2)_4I]_n$ solution, poured at the open end of the stamp, flows into microchannels by capillary forces (Figure 1a). After the complete evaporation of the solvent, the stamp is gently removed leaving the micro and nanostructures on the surface.

LCW: the stamp is gently placed in contact with a film of $[Pt_2(n\text{BuCS}_2)_4I]_n$ solution spread on the substrate and the capillary forces pin the solution to the stamp protrusions, giving rise to an array of menisci (Figure 1b). After the complete evaporation of the solvent, the stamp is gently removed leaving the micro and nanostructures on the surface.

Characterization: Optical micrographs were recorded with a Nikon i-80 microscope equipped with epiilluminator, dark-field and cross polars using 50X objective. AFM images were recorded with a commercial AFM (NT-MDT, Moscow, Russia) operating in semi-contact mode in ambient condition. Si_3N_4 cantilevers, with typical curvature radius of a tip 10 nm were used. Image analysis was done using the open source SPM software Gwyddion-www.gwyddion.net. SEM images were collected using an S- 4000 (Hitachi) instrument.

Scanning Electron Microscopy

The Scanning Electron Microscopy (SEM) images were obtained with a ZEISS 1530 SEM equipped with a Schottky emitter and operating at 10 keV. The instrument was equipped with an Energy Dispersive X-Ray Spectrometer (EDX) for X-Ray microanalysis, and two different Secondary Electrons (SE) detectors, the InLens (IL) and the Everhart-Thornley detectors (ETD). The IL detector collected a secondary electrons component (the so-called SE1) generated by the primary incident beam in a small region around the beam impinging point, and for this reason it shows an higher sensibility to surface morphology. The ETD collects the complete SE spectrum, the SE1 component, but also the SE generated by the back scattered electrons (BSE) emitted by the specimen (SE2) and the SE generated by the BSE colliding with the chamber of the instrument (SE3). In addition ETD acts also as a BSE detector with a rather low

efficiency. Therefore the detected signal shows a reduced sensitivity to the local surface morphology, but a higher sensitivity to the density and/or compositional variations.

Electrical characterization

The mobility in the saturation regime (μ_{sat}) was calculated using the equation $I_{DS} = (W/2L)C_i\mu sat(V_G–V_{th})^2$, where C_i is the capacitance of the insulating SiO_2 layer and V_{th} is the threshold voltage extracted from the square root of the drain current ($I_{DS}^{0.5}$) *versus* gate voltage (V_G) characteristics for a fixed drain voltage (V_{DS}). The OFET devices were measured in atmospheric conditions.

Acknowledgements

This work was supported by the MICINN (MAT2007-66476- C02-01/02, MAT-2010-17720 and ACI2009-0969, and PLE2009- 0065), Comunidad de Madrid (CAM2009-S2009-MAT-1467), GHJ-PLE2009-0065. MC and DG are supported by ESFEURYI DYMOT. We are grateful to Dr C. M. Pradier for help with infrared measurements and to J. Sobrado for technical support during XPS measurements at CAB.

References

1. Z. Nie, A. Petukhova and E. Kumacheva, Nat. Nanotechnol., 2010, 5, 15–25.

2. A. Martinez-Otero, E. Evangelio, R. Alibes, J. L. Bourdelande, D. Ruiz-Molina, F. Busque and J. Hernando, Langmuir, 2008, 24, 2963–2966.

3. J.-M. Lehn, Supramolecular Chemistry, VCH, Weinheim, 1995.

4. M. Cavallini, J. Mater. Chem., 2009, 19, 6085–6092.

5.M. Cavallini, I. Bergenti, S. Milita, J. C. Kengne, D. Gentili, G. Ruani, I. Salitros, V. Meded and M. Ruben, Langmuir, 2011, 27, 4076–4081.

6. D. A. Serban, P. Greco, S. Melinte, A. Vlad, C. A. Dutu, S. Zacchini, M. C. Iapalucci, F. Biscarini and M. Cavallini, Small, 2009, 5, 1117– 1122.

7. J. A. Theobald, N. S. Oxtoby, M. A. Phillips, N. R. Champness and P. H. Beton, Nature, 2003, 424, 1029–1031.

8. D. J. L. Tranchemontagne, Z. Ni, M. O'Keeffe and O. M. Yaghi, Angew. Chem., Int. Ed., 2008, 47, 5136–5147.

9. H. K. Chae, D. Y. Siberio-Perez, J. Kim, Y. Go, M. Eddaoudi, A. J. Matzger, M. O'Keeffe and O. M. Yaghi, Nature, 2004, 427, 523–527.

10. Y. You, H. Yang, J. W. Chung, J. H. Kim, Y. Jung and S. Y. Park, Angew. Chem., Int. Ed., 2010, 49, 3757–3761.

11. T. Uemura, N. Yanai and S. Kitagawa, Chem. Soc. Rev., 2009, 38, 1228–1236.

12.L. Ma, C. Abney and W. Lin, Chem. Soc. Rev., 2009, 38, 1248– 1256.

13. L. J. Murray, M. Dinca and J. R. Long, Chem. Soc. Rev., 2009, 38, 1294–1314.

14. J. Lee, O. K. Farha, J. Roberts, K. A. Scheidt, S. T. Nguyen and J. T. Hupp, Chem. Soc. Rev., 2009, 38, 1450–1459.

15. S. Kitagawa, R. Kitaura and S. Noro, Angew. Chem., Int. Ed., 2004, 43, 2334–2375.

16. C. Janiak, Dalton Trans., 2003, 2781–2804.

17. R. Mas-Balleste, J. Gomez-Herrero and F. Zamora, Chem. Soc. Rev., 2010, 39, 4220–4233.

18. L. Welte, A. Calzolari, R. Di Felice, F. Zamora and J. Gomez- Herrero, Nat. Nanotechnol., 2010, 5, 110–115.

19. A. Guijarro, O. Castillo, L. Welte, A. Calzolari, P. J. S. Miguel, C. J. G_omez-Garc_ıa, D. Olea, R. di Felice, J. G_omez-Herrero andF. Zamora, Adv. Funct. Mater., 2010, 20, 1451–1457.

20. L. Welte, U. Garc_ıa-Couceiro, O. Castillo, D. Olea, C. Polop, A. Guijarro, A. Luque, J. M. G_omez-Rodr_ıguez, J. G_omez-Herrero and F. Zamora, Adv. Mater., 2009, 21, 2025–2028.
21. M. Cavallini, C. Albonetti and F. Biscarini, Adv. Mater., 2009, 21, 1043–1053.
22. R. Mas-Balleste, R. Gonzalez-Prieto, A. Guijarro, M. A. Fernandez- Vindel and F. Zamora, Dalton Trans., 2009, 7341–7343.
23. E. Kim, Y. N. Xia and G. M. Whitesides, Nature, 1995, 376, 581– 584.
24. M. Cavallini and F. Biscarini, Nano Lett., 2003, 3, 1269–1271.
25. M. Cavallini, P. D'Angelo, V. Vendrell Criado, D. Gentili, A. Shehu, F. Leonardi, S. Milita, F. Liscio and F. Biscarini, Adv. Mater., 2011, 23, 5091–5097.
26. P. Greco, M. Cavallini, P. Stoliar, S. D. Quiroga, S. Dutta, S. Zachini, M. C. Lapalucci, V. Morandi, S. Milita, P. G. Merli and F. Biscarini, J. Am. Chem. Soc., 2008, 130, 1177–1182.
27. T. Kawamura, T. Ogaawa, T. Yamabe, H. Masuda, T. Taga, Inorg. Chem. 1987 ,26, 3547-3550.